Low-temperature molten salt synthesis and catalytic mechanism of CoS_2/NC toward advanced bifunctional electrocatalyst

Yuankun Tu[1], Chuanhua Li[1,2,3] *, Yubao Shi[1], Yu Jiang[1], Wei Xiao[1], Shenghua Zhu[1,3], Peng Lv[3], Xuemin Yan[1]*

[1] College of Chemistry and Environmental Engineering, Yangtze University, Jingzhou, 434023 Hubei, PR China

[2] State Key Laboratory of Advanced Technology for Materials Synthesis and Processing, Wuhan University of Technology, Wuhan 430070, PR China

[3] State Key Laboratory of High-efficiency Utilization of Coal and Green Chemical Engineering, Ningxia University, Yinchuan 750021, PR China

*Corresponding author

E-mail address: lichuanhuakg@126.com; xueminyan@126.com

Electrochemical measurement

To obtain the catalyst ink, mixture of 1 mL of deionized water and isopropanol (in a 1 : 9 volume ratio) was used to disperse 5 mg of catalyst and 20 μL of 5 wt% nafion solution. Then, 20 μL of catalyst ink was applied to the surface of RDE (5 mm in diameter, 0.196 cm^{-2}) in three drops to dry naturally. The RDE electrode was loaded with 0.1 mg catalyst (0.5 mg cm^{-2}). In contrast, Pt/C and IrO_2 catalyst inks were also prepared using the same process.

ORR tests were performed using the 0.1 M KOH solution with scan rate of 5 mV s^{-1}. Measurements were taken for the samples at various rotational speeds (ranging from 400 to 2000 rpm), in -0.8 ~ 0.2 V (vs. Hg/HgO) within the range of linear scanning voltammetry (LSV) curves. The cyclic voltammetry (CV) measurements were scanned at 50 mV s^{-1}. The current time chronoamperometric curves (I-T) was tested at -0.3 V (vs. Hg/HgO).

OER activity was studied using the 1 M KOH solution with LSV curves in the potential range of 0 ~ 1.0 V. The double-layer capacitance of the catalyst was estimated by CV measurements of the non-Faraday current region within potential window of 1.00 ~ 1.10 V. These tests were performed at scan rates of 20, 40, 60, 80, 100 and 120 mV s^{-1}. Electrochemical impedance spectroscopy (EIS) measurements were carried out at 1.05 V vs. RHE in the frequency range of 10^6 Hz ~ 1 Hz with an AC voltage of 10 mV. The current time chronoamperometric curves (I-T) was tested at 0.6 V (vs. Hg/HgO).

The potentials reported in this study were calibrated with reference to the reversible hydrogen electrode (RHE) using the following equation:

$$E_{vs.RHE} = E_{vs.Hg/HgO} + 0.059\ pH + 0.098 \quad (1)$$

The overpotential value for OER was calculated using the following equations.

$$\eta(V) = E_{vs.RHE} - 1.23 \quad (2)$$

The electron transfer number (n) in ORR process is calculated by Kouteckye-Levich (K-L) equations according to ORR polarization curves at different rotation speeds:[1]

$$i_d^{-1} = i_k^{-1} + i_{dl}^{-1} \quad (3)$$

$$i_k^{-1} = nFAkC_{O_2} \quad (4)$$

$$i_{dl}^{-1} = (0.62nFC_{O_2}D_{O_2}^{2/3}\nu^{-1/6})^{-1}\omega^{-1/2} \quad (5)$$

where i_d^{-1}, i_k^{-1} and i_{dl}^{-1} represent the current density of disk, kinetic and diffusion-limiting. n, F and ω is the abbreviation of overall electron transfer number per oxygen molecule, faraday constant (96485 C mol^{-1}), rotating speed of disk electrode, respectively. C_{O_2}, D_{O_2} and ν are saturated oxygen concentration (1.2×10^{-6} mol cm^{-3}), diffusion coefficient of oxygen (1.9×10^{-5} cm^2 s^{-1}) and kinematic viscosity of the electrolyte (0.01 cm^2 s^{-1}) in aqueous solution with 0.1 M KOH.

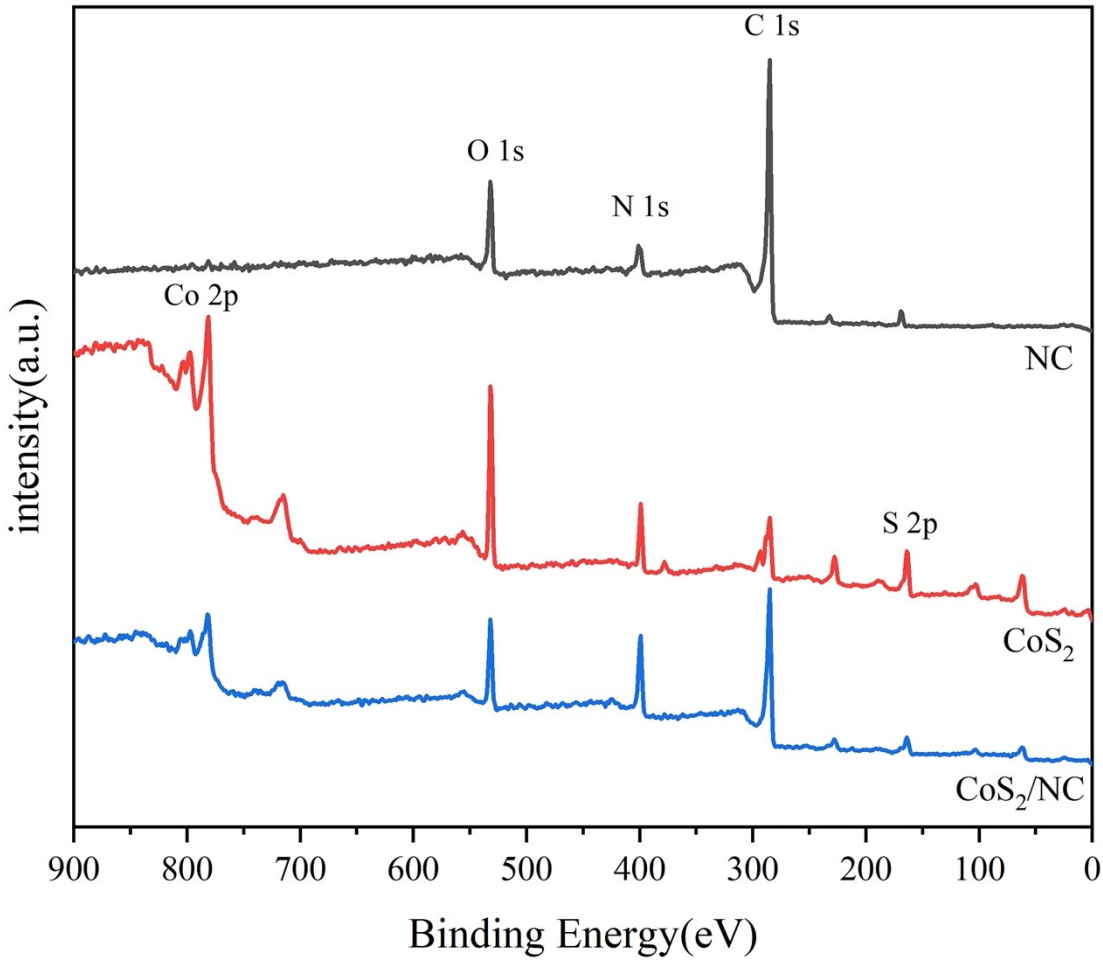

Fig.S1 Full XPS spectra of NC, CoS_2 and CoS_2/NC.

Table S1 The proportion of different nitrogen species in the N1s XPS spectra.

sample	Pyridinic N (At.%)	PyrrolicN (At.%)	Graphitic N (At.%)
NC	21.14	33.49	45.37
CoS_2/NC	32.38	17.76	49.86

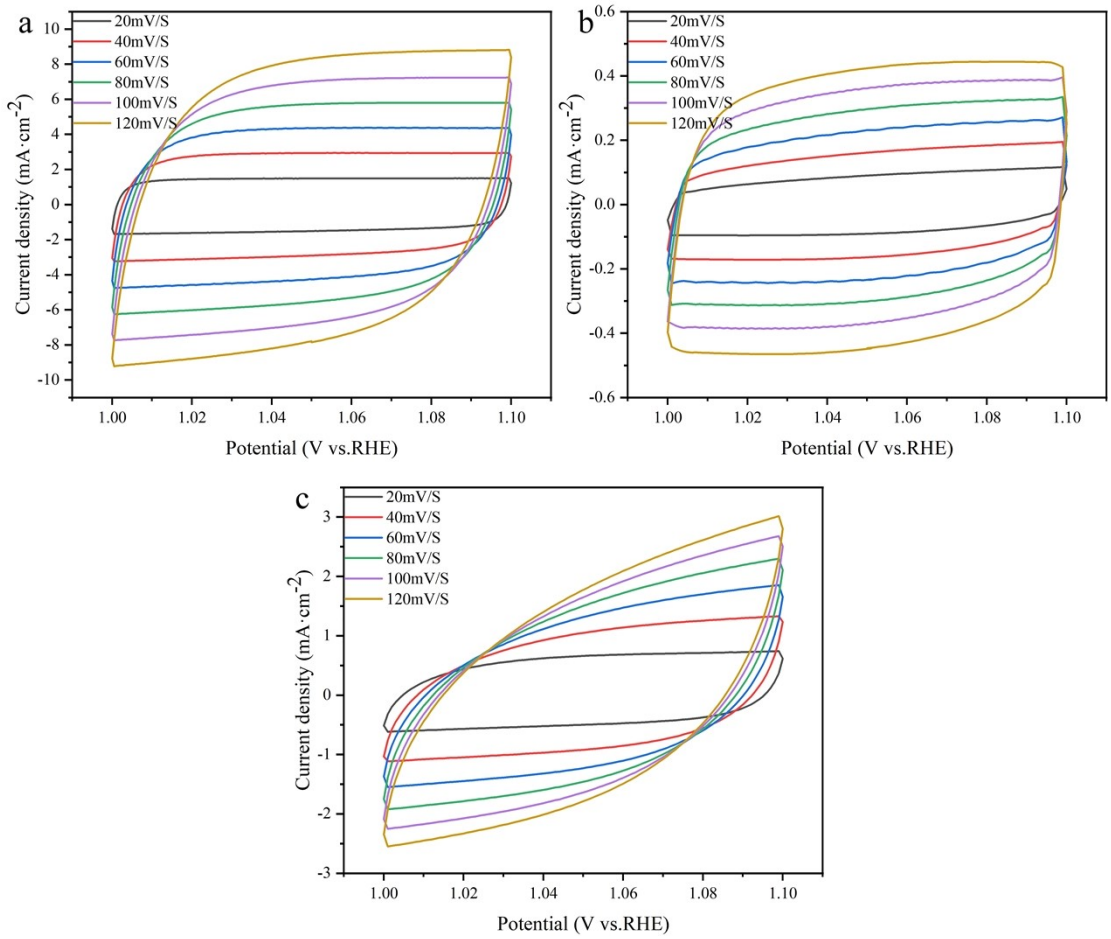

Fig.S2 CV curves for NC(a), CoS_2(b) and CoS_2/NC(c) catalysts at different scan rates of 20~120mV s^{-1} in the potential range of 1.00~1.10 V (vs. RHE).

The electrochemical active surface area (ECSA) is measured via a double layer capacitance (C_{dl}) method.[2,3] In the non-Faradaic potential region, the measured current via CV is attributed to double-layer charging current (i_c), which is equal to the product of scan rate (v) and double layer capacitance (C_{dl}), as expressed by equation:

$$i_c = vC_{dl} \quad (6)$$

Thus, a plot of a series of "i" voltammetry as a function of "v" yields a straight line whose slope is C_{dl}. The electrochemical active area of the catalyst is calculated according to equation:

$$ECSA=C_{dl}/C_s \quad (7)$$

Where the C_s is the specific capacitance of planar surface. In this work, a typical C_s value of 0.040 mF cm^{-2} in 1.0 M KOH solution is adopted for

the estimation of ECSA.[4]

For the determination of C_{dl}, CV curves were measured in a potential range of 1.00 ~ 1.10 V at scan rates of 20, 40, 60, 80, 100 and 120 mV s^{-1}. The CV curves of NC, CoS_2 and CoS_2/NC recorded at various scan rates are shown in Fig. S2. The anodic currents (i_a) and cathodic currents (i_c) at 1.05 V were extracted for further analysis. C_{dl} was then obtained by plotting i, $0.5(i_a - i_c)$, as a function of scan rate, and the results were shown in Fig. 6c. The C_{dl} of NC, CoS_2 and CoS_2/NC are determined to be 12.894, 0.667 and 2.296 mF, respectively. Accordingly, the ECSA is calculated to be 322.35 cm^2 for NC, 16.68 cm^2 for CoS_2, and 57.4 cm^2 for CoS_2/NC.

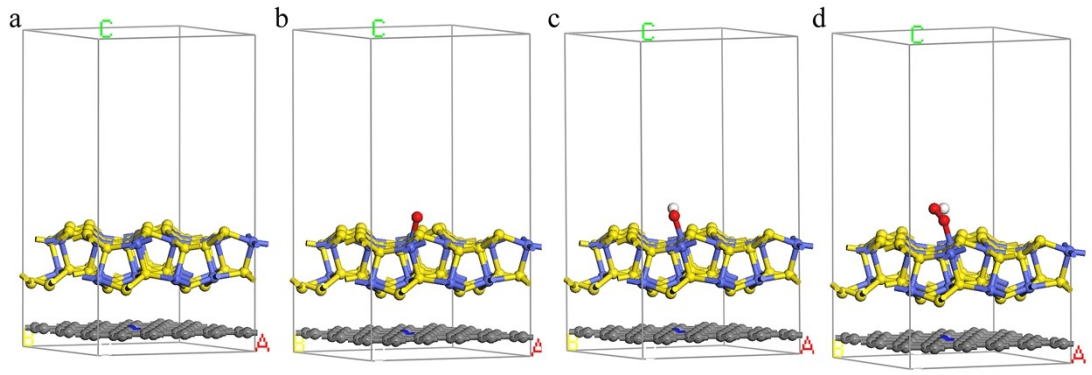

Fig.S3 The atomic models of *(a), O*(b), OH*(c) and OOH*(d) intermediates adsorbed on CoS_2/NC catalysts after geometry optimization.

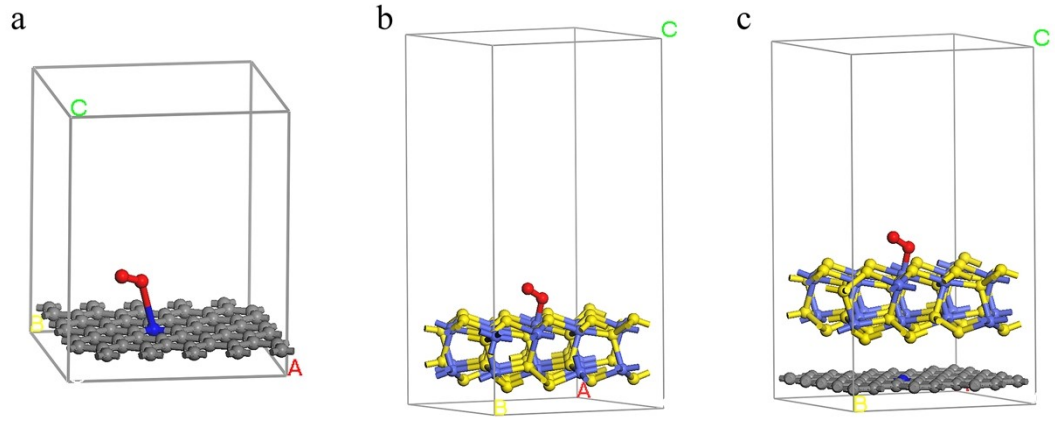

Fig.S4 The atomic models of O_2 adsorbed on (a) NC, (b) CoS_2(001) and (c) CoS_2/NC after geometry optimization.

The free energy changes for all elementary reactions in ORR are calculated according to simulated atomic model of NC, CoS_2 and CoS_2/NC. The ORR elementary reaction of 4-electron reaction pathway in an alkaline electrolyte is thought as follows:[5]

$$O_2 + {}^* + H_2O + e^- \rightarrow OOH^* + OH^- \quad (8)$$

$$OOH^* + e^- \rightarrow O^* + OH^- \quad (9)$$

$$O^* + H_2O + e^- \rightarrow OH^* + OH^- \quad (10)$$

$$OH^* + e^- \rightarrow OH^- + {}^* \quad (11)$$

where * represents bare catalyst. O*, OH* and OOH* represent that catalyst adsorbs intermediate products, such as OOH, O, and OH, respectively. The oxygen

evolution reaction (OER) is the reverse reaction of the oxygen reduction reaction (ORR), and the OER process that occurs according to four electrons is shown below:

$$OH^- + {}^* \rightarrow OH^* + e^- \quad (12)$$

$$OH^* + OH^- \rightarrow O^* + H_2O + e^- \quad (13)$$

$$O^* + OH^- \rightarrow OOH^* + e^- \quad (14)$$

$$OOH^* + OH^- \rightarrow O_2 + {}^* + H_2O + e^- \quad (15)$$

For all elementary reactions in ORR and OER, the free energy change is defined as follows:

$$\Delta G = \Delta E_{DFT} + \Delta ZPE - T\Delta S + \Delta G_{pH} - eU \quad (16)$$

where ΔE_{DFT}, ΔZPE and ΔS represent the difference of total energy, zero-point energy, and entropy between products and reactants for all elementary reactions. For ORR, the value of ΔG_{pH} is 0.769 eV at pH = 13 according to $\Delta G_{pH} = -k_B T \ln[H^+]$. U and e are the electrode potential and transferred charge, respectively. The overpotential of ORR is given by following equations (at U=0 V).

$G^{ORR} = \max\{\Delta G_1, \Delta G_2, \Delta G_3, \Delta G_4\}$, where ΔG_1, ΔG_2, ΔG_3, and ΔG_4 are calculated according to elementary reaction (8) - (11).

$$\eta^{ORR} = G^{ORR}/e + 0.461 \text{ V} \quad (17)$$

In similar way, the value of ΔG_{pH} is 0.828 eV at pH = 14. The overpotential of OER is given by following equations (at U=0 V)

$G^{OER} = \max\{\Delta G_5, \Delta G_6, \Delta G_7, \Delta G_8\}$, where ΔG_5, ΔG_6, ΔG_7, and ΔG_8 are calculated according to elementary reaction (12) - (15).

$$\eta^{OER} = G^{OER}/e - 0.402 \text{ V} \quad (18)$$

In addition, the oxygen adsorption energy of NC, CoS_2 and CoS_2/NC is given by following equations.

$$E_{ads-O_2} = E_{O_2/slab} - E_{slab} - E_{O_2} \quad (19)$$

Table S2 Catalytic performance comparison of CoS_2/NC with the recently reported CoS_2 and carbon based ORR catalysts

Catalysts	$E_{1/2}$（V）	Reference
CoS_2/NSCNTs	0.80	6
CoO/CoS_2	0.78	7
Co-CoO_X/Co-N-C	0.81	8
CoS_2/NSC-MC	0.84	9
CoS_2@MoS_2@NiS_2	0.80	10
FeS_2–CoS_2/NCFs	0.81	11
CNT–CoS_2–Fe/NC	0.80	12
LiET-CoS_2	0.82	13
Fe-SAC/NC	0.84	14
Fe@FeSA-N-C-900	0.83	15
CoS_2@NC-400	0.82	16
The N,P/CoS_2@TiO_2 NPFs	0.81	17
CoS_2/NC	0.85	This work

Table S3 Catalytic performance comparison of CoS_2/NC with the recently reported CoS_2 and carbon based OER catalysts

Catalysts	η_{10}（mV）	Reference
FeS_2/CoS_2/NSCNTs	225	6
CoS_2/NCFs	400	11
The N,P/CoS_2@TiO_2 NPFs	260	17
NC/CoS_2	380	18
CoS_2-C@MoS_2-25	390	19
CoS_2@BP-COP	270	20
CoS_2	310	21
CoS_2/NSG	393	22
N-doped CoS_2	290	23
Co-N-C-TET	280	24
CoS_2/CNT composites	290	25
EG/CoS_2-NC	335	26
CoS_2/NC	220	This work

References

1. J. Sunarso, A. A. Torriero, W. Zhou, P. C. Howlett and M. Forsyth, *The Journal of Physical Chemistry C*, 2012, **116**, 5827-5834.
2. C. C. McCrory, S. Jung, J. C. Peters and T. F. Jaramillo, *Journal of the American Chemical Society*, 2013, **135**, 16977-16987.
3. H. Wang, X. Xiao, S. Liu, C.-L. Chiang, X. Kuai, C.-K. Peng, Y.-C. Lin, X. Meng, J. Zhao and J. Choi, *Journal of the American Chemical Society*, 2019, **141**, 18578-18584.
4. Y. Ge, Y. Wu, L. Ma, X. J. Li, M. Román, R. R. Chianelli, B. Torres and D. Villagrán, *International Journal of Hydrogen Energy*, 2022, **47**, 27839-27847.
5. Z. Meng, S. Cai, R. Wang, H. Tang, S. Song and P. Tsiakaras, *Applied Catalysis B: Environmental*, 2019, **244**, 120-127.
6. K. W. Han, P. Dai, Y. Yang and M. Z. Wu, *Materials Research Bulletin*, 2022, **154**, 111942.
7. T. S. Qin, Y. Y. Ding, R. F. Zhang, X. P. Gao, Z. H. Tang, Y. G. Liu and D. Q. Gao, *Flatchem*, 2022, **32**, 100343.
8. L. H. Xu, K. K. Lu, J. J. Li and D. Shan, *Chemcatchem*, 2020, **12**, 3082-3087.
9. W. Wang, L. Q. Li, J. Ouyang, J. L. Gong, J. Tian, L. Chen, J. L. Huang, B. H. He and Z. H. Hou, *Chinese Chemical Letters*, 2023, **34**, 107597.
10. X. Liu, Z. H. Yin, M. Cui, L. G. Gao, A. M. Liu, W. N. Su, S. R. Chen, T. L. Mac and Y. Q. Li, *Journal of Colloid and Interface Science*, 2022, **610**, 653-662.
11. X. J. Shi, B. B. He, L. Zhao, Y. S. Gong, R. Wang and H. W. Wang, *Journal of Power Sources*, 2021, **482**, 228955.
12. K. Y. Hung, S. Hosseini, T. E. Ko, C. M. Tseng and Y. Y. Li, *Fuel*, 2022, **316**, 123328.
13. W. W. Zhao, P. Bothra, Z. Y. Lu, Y. B. Li, L. P. Mei, K. Liu, Z. H. Zhao, G. X. Chen, S. Back, S. Siahrostami, A. Kulkarni, J. K. Norskov, M. Bajdich and Y. Cui, *Acs Applied Energy Materials*, 2019, **2**, 8605-8614.
14. J. W. Hu, D. Y. Wu, C. Zhu, C. Hao, C. C. Xin, J. W. Zhang, J. Y. Guo, N. N. Li, G. F. Zhang and Y. T. Shi, *Nano Energy*, 2020, **72**, 104670.
15. W. J. Zhang, K. C. Fan, C. H. Chuang, P. R. Liu, J. Zhao, D. C. Qi, L. B. Zong and L. Wang, *Journal of Energy Chemistry*, 2021, **61**, 612-621.
16. Y. Zhan, S. Z. Yu, S. H. Luo, J. Feng and Q. Wang, *Acs Applied Materials & Interfaces*, 2021, **13**, 17658-17667.
17. L. Guo, J. Deng, G. Wang, Y. Hao, K. Bi, X. Wang and Y. Yang, *Advanced Functional Materials*, 2018, **28**, 1804540.
18. C. Yang, Y. X. Chang, H. Y. Kang, Y. R. Li, M. M. Yan and S. L. Xu, *Applied Physics a-Materials Science & Processing*, 2021, **127**, 465.
19. Y. Zhu, L. F. Song, N. Song, M. X. Li, C. Wang and X. F. Lu, *Acs Sustainable Chemistry & Engineering*, 2019, **7**, 2899-2905.
20. Q. Ma, R. F. Liao, Y. H. Lu, S. H. Liu, Y. C. Tang, Y. L. Zhu and D. C. Wu, *Chemistry-an Asian Journal*, 2021, **16**, 3102-3106.

21. F. Luan, S. Zhang, D. D. Chen, K. Zheng and X. M. Zhuang, *Talanta*, 2018, **182**, 529-535.
22. B. H. Chen, Z. Q. Jiang, L. S. Zhou, B. L. Deng, Z. J. Jiang, J. L. Huang and M. L. Liu, *Journal of Power Sources*, 2018, **389**, 178-187.
23. W. Yang, Z. G. Chen and H. M. Li, *International Journal of Electrochemical Science*, 2020, **15**, 1169-1186.
24. A. Samanta and C. R. Raj, *Chemelectrochem*, 2020, **7**, 2877-2887.
25. R. Nivetha, P. Kollu, K. Chandar, S. Pitchaimuthu, S. K. Jeong and A. N. Grace, *Rsc Advances*, 2019, **9**, 3215-3223.
26. J. H. Cao, C. J. Lei, B. Yang, Z. J. Li, L. C. Lei, Y. Hou and X. L. Feng, *Batteries & Supercaps*, 2019, **2**, 348-354.